Available online at www.sciencedirect.com

SCIENCE DIRECT®

Earth and Planetary Science Letters 226 (2004) 293–304

EPSL

www.elsevier.com/locate/epsl

Thermal modeling of subducted plates: tear and hotspot at the Kamchatka corner

Anne Davaille[a,*], Jonathan M. Lees[b]

[a]*Laboratoire de Dynamique des Systemes Geologiques, Institut de Physique du Globe de Paris, 4 Place Jussieu, Paris cedex 0575252, France*
[b]*Department of Geological Sciences, University of North Carolina, Chapel Hill, NC, United States*

Received 1 March 2004; received in revised form 8 July 2004; accepted 16 July 2004
Available online 11 September 2004
Editor: S. King

Abstract

Pacific plate subduction at the Aleutian–Kamchatka juncture, or corner, could be accommodated by either a large bend or a tear in the oceanic lithosphere. In this paper, we describe a number of observations which suggest that the Pacific plate terminates abruptly at the Bering transform zone (TZ). Seismicity shoals along the subduction zone from Southern Kamchatka (600 km) to relatively shallow depths near the Kamchatka–Bering Fault intersection (100–200 km). This seismicity shoaling is accompanied by an increase in the heat flow values measured on the Pacific plate. Moreover, unusual volcanic products related to adakites are erupted on Kamchatka peninsula at the juncture. Simple thermal modeling shows that a slab torn and thinner along the northern edge of the Pacific plate would be compatible with the observations. Delayed thickening of the lithosphere due to the Meiji–Hawaiian hotspot may be responsible for the required thinning.
© 2004 Published by Elsevier B.V.

Keywords: subduction; dynamics of lithosphere and mantle; hotspot

1. Introduction

While the Aleutian and Kamchatka arcs have both been explored in some detail from geophysical and geochemical perspectives, the connection at depth between the two arcs has not been addressed in detail. How can the Pacific plate, which is subducting at an oblique angle in the western Aleutians [1], physically connect to the relatively steeply dipping Kamchatka slab to the west? The surficial manifestation of the connection is the massive Bering transform zone (TZ), extending from Attu Island westward towards Kamchatka (Fig. 1). In Kamchatka the margin between the Pacific plate and North America takes a sharp turn southwards, towards the Kurile trench and Japan. How does the Pacific plate accommodate this sharp apparent bend? Does the Pacific plate drape over the corner as a tablecloth folds around a table

* Corresponding author. Tel.: +33 1 44 27232238; fax: +33 1 44 272481.
E-mail addresses: davaille@ipgp.jussieu.fr (A. Davaille), jonathan_lees@unc.edu (J.M. Lees).

0012-821X/$ - see front matter © 2004 Published by Elsevier B.V.
doi:10.1016/j.epsl.2004.07.024

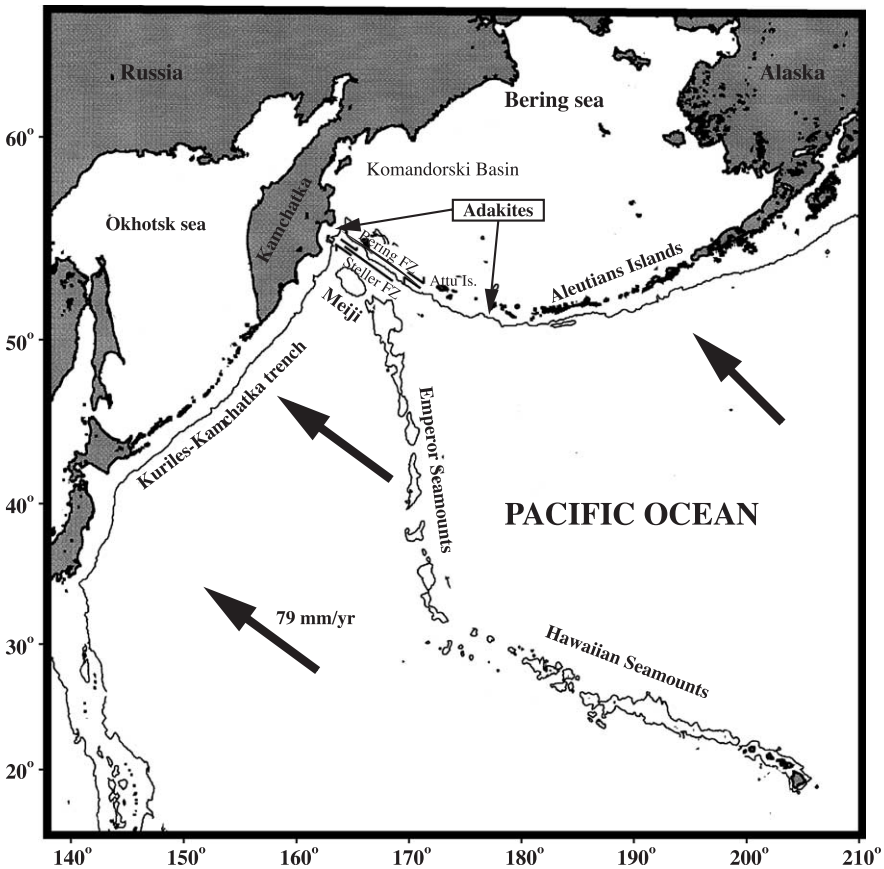

Fig. 1. Map view of the northwest Pacific. The 3000-m depth contour from the ETOPO5 database outlines the Pacific plate boundaries and the Meiji–Emperor–Hawaiian chain starting east of the Kamchatka subduction region. The Bering transform zone comprehends the Steller and the Bering faults extending from Kamchatka to east of Attu Island. The arrows show the present-day Pacific plate motion. High heat flux values are found on and around Meiji seamount [7,8].

corner, or is the Pacific plate torn at the corner along the TZ to accommodate the deformation (e.g., [2])? In this paper we explore evidence and implications for the latter hypothesis (Fig. 2). Section 2 describes the observations (seismicity, heat flow, geochemistry and tectonics) which suggest that the Pacific plate terminates abruptly at the Bering TZ. In Section 3, we use a succession of simple thermal models to show that the slab should be torn and thinner along the TZ to explain the earthquake and heat flow data. Because this thinner part of the slab lies under the beginning of the Meiji–Hawaiian hotspot track, we evaluate in Section 4 the different hotspot-related mechanisms which could be responsible for thinning.

2. Observations

Subduction under the Kurile–Kamchatka arc started 45 My ago. Old lithosphere, with ages ranging from 90 My at the trench to 80 My at the transition zone [3], subducts at an average dip angle of 49°, and a convergence rate of 7.9 cm/year, in a Northwest direction parallel to the trend of the far western Aleutian Arc [4] (Fig. 1). Seaward and to the North, the old, thick Pacific plate is separated from the relatively young Komandorsky basin by a transform boundary where transcurrent motion is distributed on two major strike–slip faults bordering both sides of the Aleutian volcanic arc [5]. The Steller (nearly coincident with the Aleutian trench) and the Bering

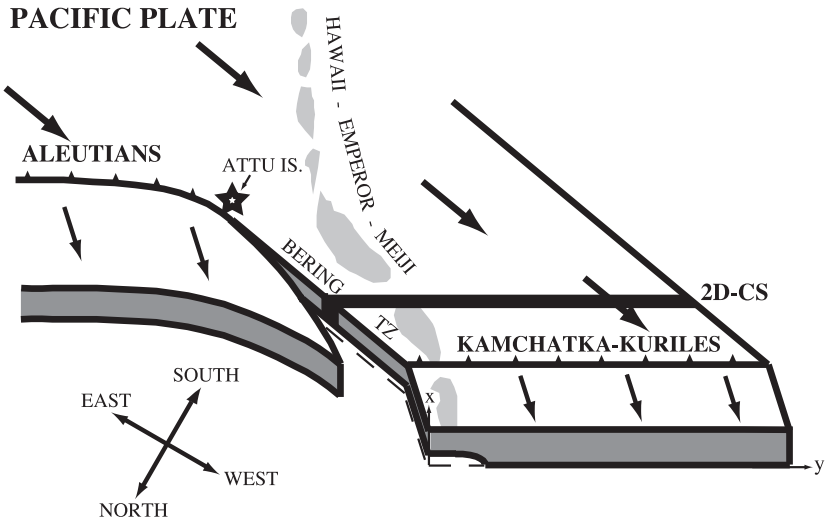

Fig. 2. Cartoon of the Pacific plate tear between the Kamchatka and Aleutian arcs, starting at Attu island. In gray is the Hawaiian hotspot track. A cross-section of the Pacific plate ("2D-CS") is outlined by the thick black line. The thermal history of this cross-section, as it enters the trench, is modeled in the text.

(to the North of the arc) faults extend over 1000 km in the Northwest Pacific and, according to plate tectonic reconstructions, have been active for more than 15 My [6]. Islands along this transform zone undergo a significant amount of shear along strike, consistent with seismicity in that region, and are transported westward [6]. Where the Bering TZ intersects with Kamchatka, strong tectonic collisional deformation is observed [5]. North of the Bering Fault, there is no evidence for ongoing subduction. Heat flux gradients are steep across the transform zone, with mean heat flow values as high as 135 mW/m^2 in the Komandorsky Basin [7], compared to mean values ranging from 68 mW/m^2 (Meiji seamount) to 48 mW/m^2 (basin) on the Pacific plate [8].

About 3% in volume of the present-day worldwide land volcanism is produced at the Kamchatka–Aleutian juncture [9] and its composition is complex. While most Kamchatka arc volcanoes are andesitic, the western Aleutian arc volcanoes exhibit unusual geochemical signatures, called adakites (high Sr, Cr, La/Yb, Sr/Y), attributed to slab melts extruded at the surface [10]. For the slab crust to be hot enough to melt requires that it be young [11] or that it resides a long time in the mantle (e.g., slow and/or shallow subduction). Adakites and similarly unusual volcanic products are observed at Sheveluch Volcano, the northern most active volcano in the Kamchatka chain [12,13]. Sheveluch Volcano differs considerably from the Kliuchevskoi group located 20 km to the south (Fig. 3), spanning the boundary where the Aleutian arc intersects with Kamchatka [14,15]. The Sheveluch–Kliuchevskoi geochemical boundary, coinciding with the on-land projection of the Bering TZ is consistent with the tear hypothesis: the edge of the subducting Pacific plate is thus exposed to the mantle, creating an opportunity for slab components to melt and mix with mantle melts as they rise to the surface.

Although global tomography offers only a crude picture of the three-dimensional (3D) structure in the upper mantle, cross-sections through the southern edge of Kamchatka differ significantly from those observed in the north [16,17]. In the south, the high-velocity slab appears to be dipping westward and extends to depths of 500–700 km. In the north, however, cross-sections perpendicular to subduction show a very shallow high-velocity slab, extending at most 200 km in depth (Fig. 3). The images suggest that the Pacific plate does not extend deep into the mantle where the Bering fault intersects the Arc. The analysis of Boyd and Creager [18] indicates cold material down to 300 km depth under the western Aleutians but did not extend to the Aleutian–Kamchatka juncture.

The seismicity pattern in the Kamchatka–Kurile slab exhibits a clear trend of shallowing to the

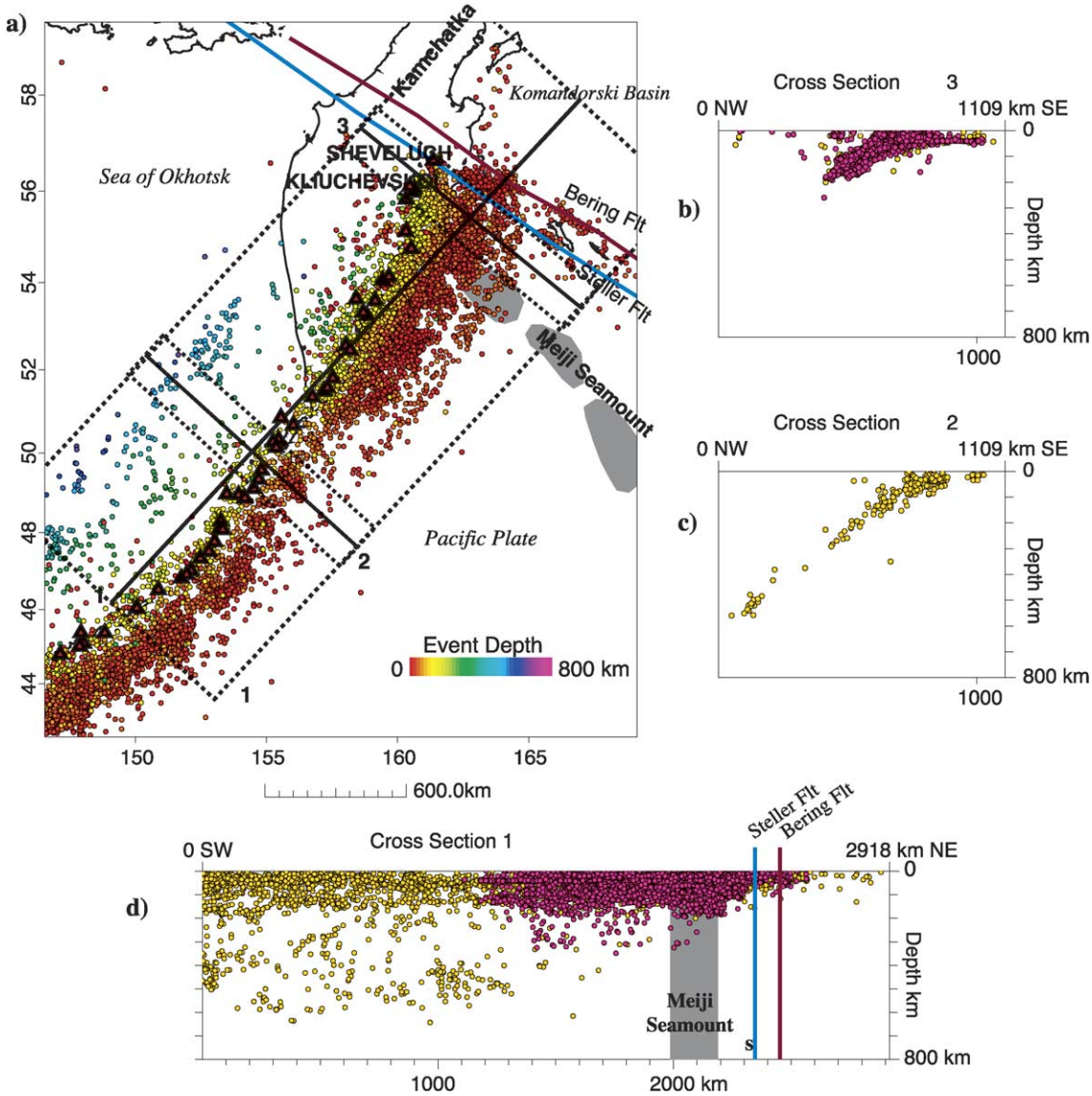

Fig. 3. Seismicity in Kamchatka. (a) Mapview showing earthquakes plotted with colors corresponding to depth. Projections of the Bering and Steller faults onto Kamchatka are presented for clarity and reference. (b–d) Vertical cross-sections of seismicity in Kamchatka. Magenta circles are from the Gorbatov et al. [3] catalog and yellow events are from the Engdahl et al. [52] catalog. The projection of the subducting Meiji seamounts is shaded gray.

north. In the Aleutians, seismicity extends along the subducting slab to relatively large depths until, in the west, subduction becomes more oblique and eventually shoals at the Bering TZ [19]. The Bering and Steller faults have seismicity extending to approximately 20–40 km with focal mechanisms dominated by strike–slip shear. In Kamchatka (Fig. 3), we observe very deep seismicity in the south extending 500–600 km that shoals to the north near the Kamchatka–Aleutian intersection. At the intersection, the deepest earthquakes are located around 50 km depth. Judging from seismicity, the subduct-

ing Pacific slab changes dip, with a shallower dip in the northern part of the Kamchatka arc [3]. The bend occurs south of the intersection of the Kamchatka Arc and the Bering TZ but north of the Meiji seamounts, as projected onto mainland Kamchatka. This change in dip may well be explained by the presence of a free slab edge at the northern corner of the plate, prolonging the TZ inland: the edge of the slab could bend upwards, lifted by the resistance of the ambient mantle to the slab's penetration.

In 1998, a broadband array of 15 seismic stations was installed in Kamchatka, extending over the whole penninsula [20]. Travel-time analysis of several teleseismic signals suggests that a high-velocity anomaly is located beneath the subducting Pacific plate, near the eastern coast of Kamchatka. In the north, however, no such anomaly is observed, reinforcing our hypothesis that the slab terminates at the Bering juncture. A study of shear wave splitting further shows an abrupt change in the fast-polarization direction, from trench-parallel, recorded on stations south of the Bering fault, to trench-normal, recorded on those located at the Bering fault and to the north [21]. This is interpreted as an abrupt change in the preferred orientation of olivine crystals in the upper mantle. The pattern of shear wave splitting therefore suggests that flow in the upper mantle is significantly controlled by the lack of a subducting slab to the north.

As summarized above, observations from different fields suggest an abrupt termination of the Pacific plate at the Bering TZ. In the absence of strong evidence for a recent plate reorganization in the area [6], the landward trace of the Pacific plate edge is the projection of the TZ (Fig. 3) and extends hundreds of kilometers into the mantle.

3. Thermal modeling

To first order, the occurrence of seismicity is constrained by the presence of cold temperatures in the slab [22–24]. The question is thus whether the reheating of the Bering TZ edge of the slab can explain the shoaling of seismicity in Kamchatka. We therefore present a succession of simple thermal models with different initial and boundary conditions to explore the different mechanisms which could explain the data.

3.1. The edge effect

We focus on the thermal evolution through time of a slab entering in the hot mantle. Up to now, reheating of a slab has been studied when the slab is infinite along the trench direction (e.g., [22,23]). We consider here the case of the conductive reheating of a semi-infinite slab, i.e., with an edge normal to the trench direction (Fig. 2). The effects of adiabatic, shear or radiogenic heating are neglected, and the thermal diffusivity coefficient is kept constant. We suppose that the subduction zone is old enough to have reached a quasi-steady state. With a rapid convergence rate V (V=7.9 cm/year in Kamchatka), the Peclet number, which measures advection versus thermal diffusion effects, $Pe=VL/\kappa$ is high (around 250 in Kamchatka), where L (=100 km) is the thickness of the slab and κ ($=10^{-6}$ m^2/s) is its thermal diffusivity. Thus, thermal conduction within the slab along the direction of plate motion can be neglected compared to conductive reheating normal to the slab [22]. The steady-state reheating of the three-dimensional (3D) slab (Fig. 2) is thus equivalent to the two-dimensional (2D) conductive reheating through time of a slab cross-section, (labelled "2D-CS" on Fig. 2), which enters at t=0 in the hot mantle at temperature T_m (Fig. 4a). We do not consider the flow in the continental mantle wedge below Kamchatka and therefore the reheating that we calculate will be an upper bound.

The lithospheric plate can be identified with the upper thermal boundary layer of the mantle, which thickens with time as it cools and moves away from the midocean ridge. Thus, the slab's internal temperature distribution is a function of its age. For a plate older than 70 My, the vertical temperature structure can be approximated by a linear gradient (Fig. 4b) because heat added to the plate from below balances heat lost at the seafloor (e.g., [22,25–27]). Because the lithosphere entering the Kamchatka trench is 90 My old [3], we take this linear profile (Fig. 4b) as our initial thermal condition.

The reheating history of the slab 2D cross-section, entering at t=0 in a hot mantle at constant temperature T_m, can then be determined analytically (Carlsraw and Jaeger [28], pp. 93–96). Using (primed) dimension-

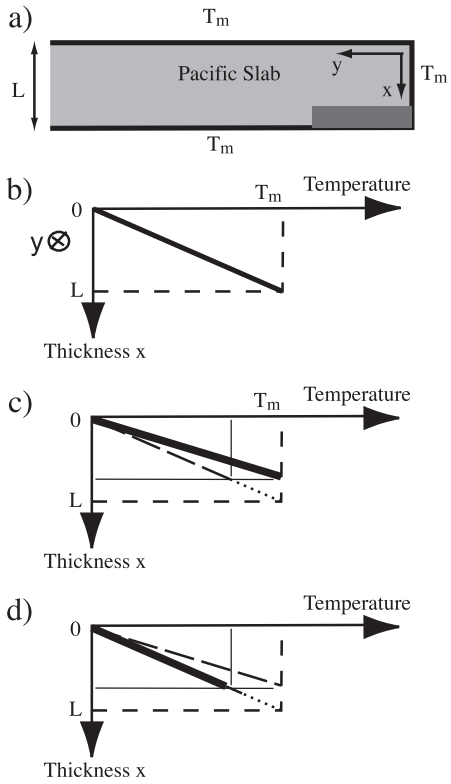

Fig. 4. (a and b) Initial thermal conditions for the different models discussed in the text: (a) Boundary conditions: for $t<0$, the upper boundary of the cross-section is in contact with the ocean, and its lower boundary is in contact with the mantle. At $t=0$, the slab cross-section plunges into the mantle at temperature T_m; dark gray color underlines the area possibly missing if the slab is thinned towards its Bering edge. (b) Thermal structure within the slab before it enters the trench. (c and d) The thick lines show the thermal structure within the slab thinner part when the slab is thinned towards its Bering edge: In (c), thinning occurs well before the trench and the temperature in the thinned part has time to equilibrate with the mantle. In (d), thinning suddenly occurs when the slab enters the trench: the hotter part of the slab is therefore removed and the remains are colder than in the previous case. The dotted line represents normal lithosphere, and the thinned lines allow comparison between cases (c) and (d).

less variables, the temporal evolution of the temperature inside the slab can be written as:

$$T(x',y',t') = 1 - \frac{2}{\pi} erf\left(\frac{y'}{2\sqrt{t'}}\right) \times \sum_{n=1}^{\infty} \frac{(-1)^{n-1}}{n} e^{-n^2\pi^2 t'} \sin(n\pi x') \quad (1)$$

The dimensionalized variables are then given by

$$t = t'L^2/\kappa, \quad x = x'L, \quad y = y'L, \quad \text{and} \quad \mathrm{T} = \mathrm{T}'\mathrm{T_m}. \quad (2)$$

At any given dimensionless time t', a given cross-section will be at a depth z, which is the product of t and the vertical descent rate:

$$z = \sin(\alpha) V t' L^2/\kappa \quad (3)$$

where α is the dip angle. Eqs. (1)–(3) give a temperature distribution typical of slab models [22–24]. The minimum temperature is initially near the upper slab surface (Fig. 5a) and moves toward the slab center with increasing time (Fig. 5b). Meanwhile, it also moves further away from the Bering edge (Fig. 5b). Fig. 6 shows the evolution through time of the minimum temperature in the slab. Successively hotter isotherms penetrate to greater depths, and temperatures at 670 km are between 600 and 700 °C, which presumably allows for deep seismicity (e.g., [24]). Reheating is faster towards the edge of the slab (Fig. 5), and the hot isotherms are accordingly shallower, but this effect is confined to a characteristic distance smaller than the thickness of the slab (Fig. 6b). The observed seismicity (Fig. 6) follows well the thermal structure near the edge for shallow seismicity (region "1" on Fig. 6b) and far from the edge for deep seismicity (region "3" on Fig. 6b). For seismicity down to 300 km, our calculated temperature at the seismicity cutoff depth is in agreement with the constant fraction of the depth-dependent mantle solidus proposed by Creager and Boyd [1] based on their Aleutian arc study. This is consistent with the idea that seismicity terminates because of the initiation of high-temperature, steady-state creep [23]. However, the edge-effect model presented above is still not sufficient to explain the lack of deep seismicity (300 to 700 km) at intermediate distances (50 to 500 km from the edge, region "2" on Fig. 6b).

Influence of the Bering TZ: One might argue that, when it enters the mantle below Kamchatka, the Pacific plate has been moving for 10–15 My along the Bering TZ and the hot Komandorsky basin. Therefore, it has been reheated from the Bering edge for a while. Hence, close to the edge, the initial thermal

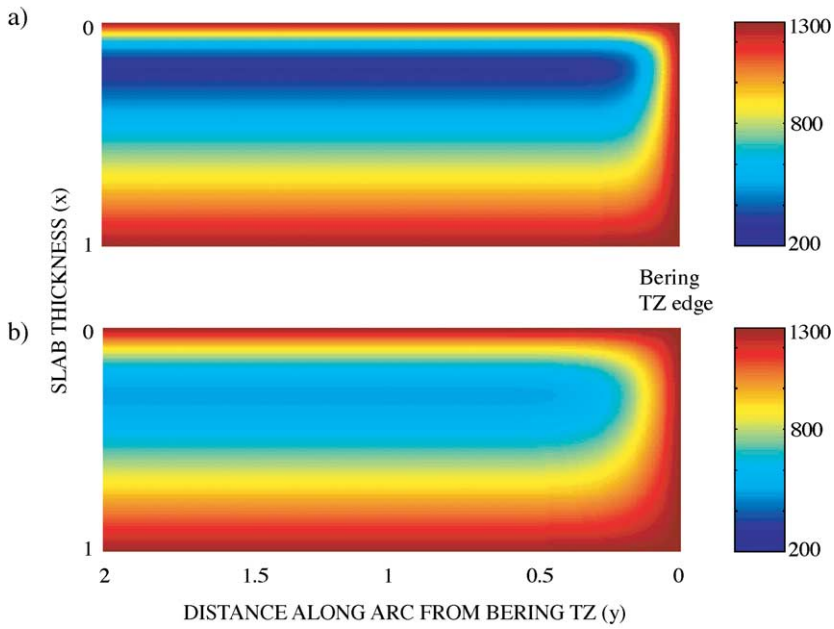

Fig. 5. Thermal structure of a cross-section of the slab calculated from Eq. (3) at two different times with the initial boundary conditions shown on Fig. 4b. (a) t=0.005 (1.6 My) and (b) t=0.015 (4.8 My).

boundary condition pictured in Fig. 4b and taken in the previous calculation is perturbed because the isotherms are moving inwards before the plate enters the subduction zone. However, the effect remains confined within a small distance of the edge of the plate (less than the thickness of the plate): this is not surprising because it is very inefficient to heat a rod by its end.

Hence, even taking into account the thermal perturbation due to the Bering TZ prior to subduction, the lack of deep seismicity under the Kamchatka corner cannot be due to an edge effect alone.

3.2. Lithosphere thinning

The lack of deep seismicity can be due either to a lack of slab material at this depth (slab loss model, i.e., [29]) or to a thinner lithosphere. We are going to show that the observations require the latter.

According to Eqs. (1)–(3), the depth attained by a given isotherm at a certain time depends only on the initial thickness of the lithosphere L. The shoaling of seismicity can thus be explained by the thinning of the plate towards the edge (e.g., [3]). Given the depth dependence of the seismicity cutoff temperature, we can invert Kamchatka seismicity data to determine the variation of the lithosphere thickness $L(y)$ along the trench. This was done numerically using a finite element code [30] because an analytical solution does not exist when the slab shape is arbitrary (Fig. 6). The actual amount of thinning depends on the depth dependence of the cutoff temperature and on the timing of the thinning. The choice of the initial boundary conditions can give us an idea of the latter.

Let us first consider that the lithosphere was thinned well before entering the trench (Fig. 6a): it can have reached thermal equilibrium and its initial thermal structure is given in Fig. 4c. If the same mechanism, and therefore the same potential isotherm, controlled earthquake occurrence down to 670 km depth (e.g., [23]), the amount of thinning required to explain the seismic data would then be around 30% (Fig. 6b). On the other hand, Kirby et al. [24] propose that two different mechanisms are responsible for shallow and deep seismicity, which may lead to two different controlling isotherms. In this case, the amount of required thinning could be reduced to 20–10%. A lower bound of the heat flux

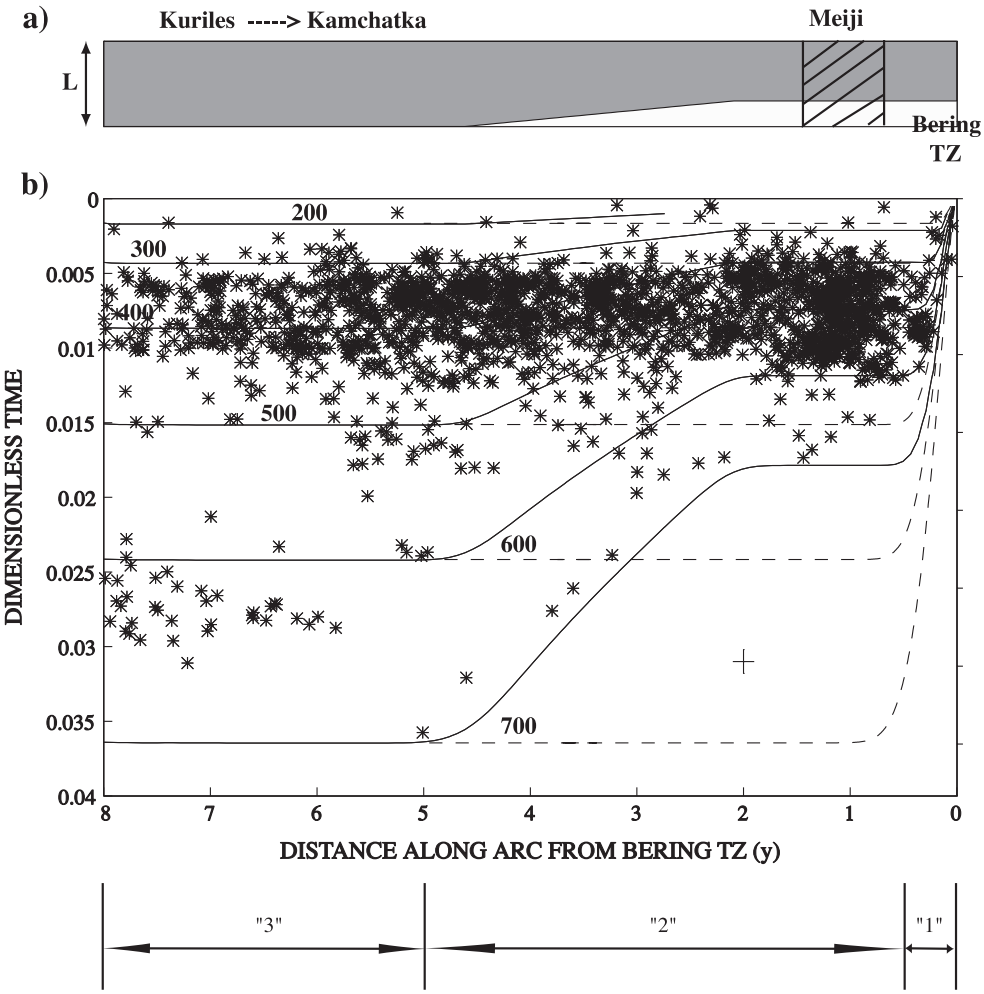

Fig. 6. (a) Shape of the cross-section of the lithosphere (cf. Fig. 2) entering the trench. (b) Isotherms and seismicity in the Kamchatka arc. The epicenters' distances down the subduction zone were corrected for Earth's curvature and converted in dimensionless time through Eq. (3), using L=100 km. The symbol (+) gives the error bars on the hypocentre locations (*). The dashed lines represent the analytical model obtained for a slab of constant thickness L. The solid lines stand for the numerical model calculated with the thinned gray slab shape in (a). "1" designates the zone sensitive to the TZ edge effect, "2" the thinner zone under the Hawaiian hotspot, and "3" the "normal" lithosphere.

can be estimated by its value at steady state which scales as:

$$Q \approx k\frac{T_{\mathrm{m}}}{L(y)} = Q_{\mathrm{plate}}\frac{L_{\mathrm{plate}}}{L(y)} \quad (4)$$

where Q_{plate} and L_{plate} are the heat flux (48 mW/m^2) and lithosphere thickness (100 km) of the "normal" Pacific plate [8,31]. A 10% thinning would therefore give a minimum heat flux on the hotspot track of 53 mW/m^2 while a 30% thinning would give 69 mW/m^2, which is consistent with the observed mean value of 68 mW/m^2 around Meiji seamount [7,8].

In the case where normal lithosphere enters the trench and is suddenly delaminated, the thinned lithosphere is colder than in the previous case (Fig. 4d). Thus, a thinning greater than 50% is then needed to explain the lack of deep seismicity. A mechanism able to produce such a thinning in so short a time remains to be found. It is probably more plausible in this case to envision the complete loss of part of the slab (i.e., [29]). However, neither catastrophic slab

loss nor sudden delamination of the slab once it has entered the trench can explain the heat flow increase observed around Meiji seamount [8] *before* the Pacific plate enters the trench. This observation alone requires a lithosphere already thinner before entering the trench, and the corresponding amount of thinning would then explain perfectly the lack of deep seismicity.

4. Hotspot, thinner lithosphere and tear

The 10–30% thinning is located under the Meiji–Emperor–Hawaii hotspot chain, 80 My downstream from the present-day active hotspot. The simplest interpretation is thus that the lithosphere is thinner there due to the impact of the Hawaiian hotspot.

Hotspot-induced thinning: Thermal rejuvenation or delayed thickening? It has long been a question whether thermal rejuvenation of a moving lithosphere could be produced by a hotspot [32], because if a thermal perturbation had to propagate upwards into the lithosphere by conduction, it would take tens of millions of years. Indeed, no significant lithospheric thinning has ever been imaged [33–35] nor modeled (e.g., [36,37]) on the active sites of fast Pacific plate hotspots. Recently, it has been shown that small-scale convection triggered by the temperature contrast between hotspot material and lithosphere [27,38,39] can accelerate the process of thermal delamination of the lithosphere. On a fast plate, thinning of the lithosphere should be observable along the hotspot track downstream of the present-day location of the hotspot. This seems to be consistent with recent results by Li et al. [40], who observed on the Hawaiian track a 30% lithospheric thinning under Kauai, 400 km downstream from the present-day active hotspot. On a much slower plate, Bonneville et al. [41] inferred from heat flow measurements a 30% thinning 36 My downstream on La Reunion hotspot track. And heat flow variations on the 140-My-old and nearly stationary Cape Verde hotspot are also compatible with a 30% lithospheric thinning [42].

Recent laboratory experiments have suggested that small-scale convection effects would be further enhanced if the plume was located close to a ridge [43]. The hot temperature anomaly due to the ridge-centered plume triggers small-scale instabilities almost at the ridge, i.e., much sooner than under a normal lithosphere. These instabilities accelerate the heat transfer out of the mantle but delay the thickening of the lithosphere as it cools and moves away from the ridge. A groove under the lithosphere is therefore expected along the track of a ridge-centered hotspot (Fig. 7). Plate reconstructions [44] and geochemistry studies (e.g., [45]) show that 80 My ago, the Hawaiian plume was on a ridge, which migrated away from it since then. The 10–30% amount of thinning inferred in Section 3 from geophysical data suggests that the plume may have indeed "grooved" the lithosphere as the ridge moved away [46,47]. We propose that delayed thickening of the lithosphere might be, in this case, a more efficient mechanism to produce a thinner lithosphere than thermal rejuvenation. Because a normal lithosphere thickens as the square root of age, at least at young ages (0–70 My, e.g., [22]), the 10–30% of thinning implies that lithosphere cooling has been delayed under the hotspot by 20–45 My. In other terms, anomalously hot plume material has been flowing under this ridge location for at least 20 to 45 My in order to impede cooling. Detailed numerical models (e.g., [37]) can give us an idea of the duration of the dynamical influence of a hotspot

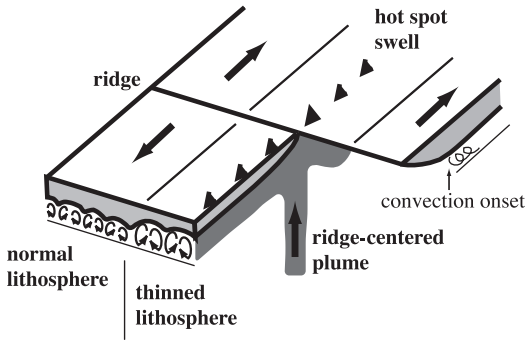

Fig. 7. Plume–ridge interaction. As the lithosphere cools away from the ridge, cold small-scale convective instabilities develop from its bottom. Sheared by the plate tectonic large-scale flow, they remain trapped in the asthenospheric mantle where the shear is strongest, giving birth, some distance from the spreading ridge, to a pattern of helices aligned in the direction of plate motion, which groove the bottom of the lithosphere. The hot temperature anomaly due to the ridge-centered plume triggers small-scale instabilities almost at the ridge, i.e., much sooner than under normal lithosphere. These small-scale instabilities accelerate the heat transfer out of the mantle but delay the thickening of the lithosphere as it moves and cools away from the ridge. This will create a channel under the lithosphere along the track of a ridge-centered hotspot.

plume on a given location of its track: they show that the swell of dynamic origin at Hawaii reaches a maximum 500 km downstream from the hotspot source and decreases significantly only $\mathcal{L} = 2500$ km downstream of the source. Thus, a given location on the track will receive hot material from the plume for at least 32 My ($= \mathcal{L}/U$). Our crude estimate of 20–45 My delay is therefore quite reasonable. Hence, we expect the Pacific lithosphere along the Bering TZ to have developed a groove along the hotspot track because the Hawaiian hotspot was, at this time, close to a ridge. Nowadays, the Hawaiian hotspot erupts on 90-My-old lithosphere, very far from any ridge. Hence, delayed thickening of the lithosphere cannot be advocated to induce lithosphere thinning, which might be a reason why such thinning has not been imaged by seismic studies on the newest part of the hotspot track [33,34,40].

Tear: It is probably not a coincidence that the massive Bering TZ runs parallel to this portion of the Hawaiian hotspot track, because the Pacific lithosphere there has been weakened by the volcanism and thinning associated with the hotspot activity: this could have helped to localize a tear and initiate a transform zone system. Plate tectonics reconstructions in the area are still controversial (see [48] for a review), and the whereabouts of the Hawaiian hotspot prior to 80 My remain unknown. However, the Meiji–Detroit part of the Hawaiian track probably reached the Aleutians subduction zone 15 My ago, being nearly parallel to the trench. If we assume that the large Bering transform fault extending from the Aleutians to Kamchatka has nucleated on the weakened Meiji–Emperor–Hawaiian track, we might speculate that the Hawaiian hotspot is older than 95 My.

5. Conclusions

Thermal modeling of the reheating of a torn slab shows that the seismic and heat flux data at the Kamchatka corner can be explained if the Pacific plate is thinner along the Hawaiian hotspot track and is torn along the Bering transform zone. This would also be compatible with geochemical data.

The heat flux data requires that the Pacific lithosphere was already thinner well before entering the trench, which may be explained by delayed thickening of the lithosphere below the Meiji–Hawaiian hotspot. The corresponding amount of thinning would then explain the lack of deep seismicity. Therefore, a slab loss [29], although possible, is not required by the data.

This study also shows that inspection of seismicity patterns in subduction zones where hotspot tracks are subducting provides another means to image and quantify plume-related lithospheric thinning. The Kamchatka–Hawaiian case is not unique: similar gaps in seismicity exist along the Kermadec–Tonga trench, in the projection of the intersection of the Louisville hotspot ridge [49], and in the trench in Ecuador where the Galapagos hotspot track enters the trench. The latter is sometimes also associated with a slab "window" or slab tear [50].

This leads to the question of the relationship between hotspot activity and faulting or tear localization. More work needs to be done to understand quantitatively as well as qualitatively the physics of those phenomena.

Acknowledgments

This work was supported under NSF grant EAR9614639 and French INSU program IDYL. It benefited from discussions with Mark Davis, Michel Diament, Bob Engdhal, Jean-Claude Mareschal and Neil Ribe, from the stimulating comments of Alain Bonneville and Dave Schott on an earlier version of the manuscript, and from thorough reviews by Magali Billen, Emile Okal, and an anonymous reviewer. We thank Claude Jaupart who provided the finite element code, and Christina Widiwiyanti who created Fig. 1 using GMT by Wessel and Smith [51].

References

[1] K.C. Creager, T.M. Boyd, The geometry of Aleutian subduction: three-dimensional kinematic flow model, J. Geophys. Res. 96 (1991) 2293–2307.

[2] K. Yamaoka, Y. Fukao, M. Kumazawa, Spherical shell tectonics: effects of sphericity and inextensibility on the geometry of the descending lithosphere, Rev. Geophys. 24 (1986) 27–55.

[3] A. Gorbatov, V. Kostoglodov, S. Gerardo, E. Gordeev, Seismicity and structure of the Kamchatka subduction zone, J. Geophys. Res. 102 (1997) 17883–17898.

[4] C. DeMets, R.G. Gordon, D.F. Argus, S. Stein, Current plate motions, Geophys. J. Int. 101 (1990) 425–478.
[5] E.L. Geist, D.W. Scholl, Large-scale deformation related to the collision of the Aleutian arc with Kamchatka, Tectonics 13 (1994) 538–560.
[6] B.V. Baranov, N.I. Seliverstov, A.V. Muravev, E.L. Uzurov, Komandorsky Basin: spreading behind a transform plate boundary, Tectonophysics 199 (1991) 237–269.
[7] Ya. B. Smirnov, V.M. Sugrobov, Terrestrial heat flow in the northwestern Pacific, Tectonophysics 83 (1982) 109–122.
[8] I.K. Tuezov, V.D. Epaneshnikov, P.Y.U. Gonnov, Heat field of the lithosphere in Northeast Asia and the Northern Sector of the Asia-Pacific transition zone, in: V. Cermak, L. Rybach (Eds.), Terrestrial Heat Flow and the Lithosphere Structure, Springer-Verlag, Berlin, 1991, pp. 238–263.
[9] S.A. Fedotov, Y.P. Masurenkov, Active Volcanoes of Kamchatka, Nauka, Moscow, 1999, p. 302.
[10] O.N. Volynets, V.V. Ponomareva, A.D. Babansky, Magnesium basalts of Sheveluch andesite volcano, Kamchatka, J. Petrol. 5 (1997) 183–196.
[11] M.J. Defant, M.S. Drummond, Derivation of some modern arc magmas by melting of young subducted lithosphere, Nature 347 (1990) 662–665.
[12] S.M. Kay, R.W. Kay, Aleutian magmas in space and time, in: G. Plafker, H.C. Berg (Eds.), Geology of Alaska, The Geology of North America, v. G-1, Geological Society of America, Boulder, 1994, pp. 687–722.
[13] G.M. Yogodzinski, O.N. Volynets, A.V. Koloskov, S.M. Kay, Magnesium andesite in the Western Aleutian Komandorsky region: implications for slab melting and processes in the mantle wedge, Bull. G.S.A. 107 (1995) 505–519.
[14] G.M. Yogodzinski, J.M. Lees, T.G. Churikova, F. Dorendorf, G. Woerner, O.N. Volynets, Geochemical evidence for the melting of subducting oceanic lithosphere at plate edges, Nature 409 (2001) 500–504.
[15] P. Kepezhinskas, F. McDermott, M.J. Defant, A. Hochstaedter, M.S. Drummond, C.J. Hawkesworth, A. Koloskov, R.C. Maury, H. Bellon, Geochim. Cosmochim. Acta 61 (1997) 577–600.
[16] J.M. Lees, M. Brandon, J. Park, V. Levin, A. Ozerov, E. Gordeev, Kamchatka: edge of the plate, IRIS Newsl. 2000 (2000) 17–19.
[17] S. Widiyantoro, R.D. van der Hilst, Mantle structure beneath Indonesia inferred from high-resolution tomographic imaging, Geophys. J. Int. 130 (1997) 167–182.
[18] T.M. Boyd, K.C. Creager, The geometry of Aleutian subduction: three-dimensional seismic imaging, J. Geophys. Res. 96 (1991) 2267–2291.
[19] E.R. Engdahl, R. van der Hilst, S.H. Kirby, G. Ekström, A global survey of slab structures and internal processes using a combined data base of high-resolution earthquake hypocenters, tomographic images and focal mechanism data, Seismol. Res. Lett. 69 (1998) 153–154.
[20] J.M. Lees, J. Park, V. Levin, V. Peyton, E. Gordeev, A. Ozerov, V. Chebrov, Side Edge of Kamchatka Slab: 1998–1999, IUGG XXII General Assembly, Abstracts IUGG XXII General Assembly, 1999, p. 157.
[21] V. Peyton, V. Levin, J. Park, M. Brandon, J. Lees, E. Gordeev, A. Ozerov, Mantle flow at a slab edge: seismic anisotropy in the Kamchatka region, Geophys. Res. Lett. 28 (2000) 379–382.
[22] D.P. McKenzie, Speculations on the consequences and causes of plate motions, Geophys. J. R. Astron. Soc. 18 (1969) 1–32.
[23] P. Molnar, D. Freedman, J.S.F. Shih, Lengths of intermediate and deep seismic zones and temperatures in downgoing slabs of lithosphere, Geophys. J. R. Astron. Soc. 56 (1979) 41–54.
[24] S.H. Kirby, S. Stein, E.A. Okal, D.C. Rubie, Metastable mantle phase transformations and deep earthquake in subducting oceanic lithosphere, Rev. Geophys. 34 (1996) 261–306.
[25] B. Parsons, D. McKenzie, Mantle convection and the thermal structure of the plates, J. Geophys. Res. 83 (1978) 4485–4495.
[26] C.A. Stein, S. Stein, A model for the global variation in oceanic depth and heat flow with lithospheric age, Nature 359 (1992) 123–129.
[27] A. Davaille, C. Jaupart, Onset of thermal convection in fluids with temperature-dependent viscosity: application to the oceanic mantle, J. Geophys. Res. 99 (1994) 19853–19866.
[28] H.S. Carlsraw, J.C. Jaeger, Conduction of Heat in Solids, Oxford Univ., Press, 1959.
[29] V. Levin, N. Shapiro, J. Park, M. Ritzwoller, Seismic evidence for catastrophic slab loss beneath Kamchatka, Nature 418 (2002) 763–767.
[30] C. Jaupart, A. Provost, Heat focussing, granite genesis and inverted metamorphic gradients in continental collision zones, Earth Planet. Sci. Lett. 73 (1985) 385–397.
[31] C.R.B. Lister, J.G. Sclater, E.E. Davis, H. Villinger, S. Nagihara, Heat flow maintained in ocean basins of great age: investigations in the north-equatorial west Pacific, Geophys. J. Int. 102 (1990) 603–630.
[32] S.T. Crough, Thermal origin of mid-plate hotspot swells, Geophys. J. R. Astron. Soc. 55 (1978) 451–469.
[33] M.T. Woods, E.A. Okal, Rayleigh-wave dispersion along the Hawaiian swell: a test of lithospheric thinning by thermal rejuvenation at a hotspot, Geophys. J. Int. 125 (1996) 325–339.
[34] K. Priestley, F. Tilmann, Shear-wave structure of the lithosphere above the Hawaiian hot spot from two-station Rayleigh wave phase velocity measurements, Geophys. Res. Lett. 26 (1999) 1493–1496.
[35] Y. Yoshida, D. Suetsugu, Lithospheric thickness beneath the Pitcairn hot spot trail as inferred from Rayleigh wave dispersion, Phys. Earth Planet. Inter. 146 (2004) 75–85.
[36] N.H. Sleep, Hotspots and mantle plumes: some phenomenology, J. Geophys. Res. 95 (1990) 6715–6736.
[37] N.M. Ribe, U.R. Christensen, The dynamical origin of Hawaiian volcanism, Earth Planet. Sci. Lett. 171 (1999) 517–531.
[38] N.H. Sleep, Lithospheric thinning by midplate mantle plumes and the thermal history of hot plume material ponded at sublithospheric depths, J. Geophys. Res. 99 (1994) 9327–9343.

[39] W.B. Moore, G. Schubert, P. Tackley, Three-dimensional simulations of plume–lithosphere interaction at the Hawaiian swell, Science 279 (1998) 1008–1011.
[40] X. Li, R. Kind, X. Yuan, I. Wölbern, W. Hanka, Rejuvenation of the lithosphere by the Hawaiian plume, Nature 427 (2004) 827–829.
[41] A. Bonneville, R.P. Von Herzen, F. Lucazeau, Heat flow over Reunion hot spot track: additional evidence for thermal rejuvenation of oceanic lithosphere, J. Geophys. Res. 102 (1997) 22731–22747.
[42] R.C. Courtney, R.S. White, Anomalous heat flow and geoid across the Cape Verde Rise: evidence for dynamic support from a thermal plume in the mantle, Geophys. J. R. Astron. Soc. 87 (1986) 815–867.
[43] C. Crambes, A. Davaille, A. Lee, J.M. Lees, Small-scale convection confined under the lithosphere, Phys. Earth Planet. Inter. (2003) (submitted).
[44] J. Mammerickx, G.F. Sharman, Tectonic evolution of the North Pacific during the cretaceous quiet period, J. Geophys. Res. 93 (1988) 3009–3024.
[45] R.A. Keller, M.R. Fisk, W.M. White, Isotopic evidence for late Cretaceous plume–ridge interaction at the Hawaiian hotpsot, Nature 405 (2000) 673–676.
[46] W.J. Morgan, Darwin Rodriguez, Amsterdam, a second type of hotspot island, J. Geophys. Res. 83 (1978) 5355–5360.
[47] J.-G. Schilling, Fluxes and excess temperatures of mantle plumes inferred from their interaction with migrating mid-ocean ridges, Nature 352 (1991) 397–403.
[48] J. Park, V. Levin, M. Brandon, J. Lees, V. Peyton, E. Gordeev, A. Ozerov, A dangling slab, amplified arc volcanism, mantle flow and seismic anisotropy in the Kamchatka corner, in: S. Stein, J.T. Freymueller (Eds.), Plate Boundary Zones, AGU Geodynamics Series, vol. 30, 2002, pp. 295–324.
[49] D. Giardini, J.H. Woodhouse, Deep seismicity and modes of deformation in Tonga subduction zone, Nature 307 (1984) 505–509.
[50] M.A. Gutscher, J. Malavielle, S. Lallemand, J.Y. Collot, Tectonic segmentation of the North Andean margin: impact of the Carnegie Ridge collision, Earth Planet. Sci. Lett. 168 (1999) 255–270.
[51] P. Wessel, W.H.H. Smith, New version of the Generic Mapping Tools released, EOS 76 (1995) 329.
[52] E.R. Engdahl, R. van der Hilst, R. Buland, Global teleseismic earthquake relocation with improved travel times and procedures for depth determination, Bull. Seismol. Soc. Am. 88 (1998) 722–743.